

Coronary disease is not associated with robust alterations in inflammatory gene expression in human epicardial fat

Timothy P. Fitzgibbons,¹ Nancy Lee,¹ Khanh-Van Tran,¹ Sara Nicoloso,² Mark Kelly,² Stanley K.C. Tam,³ and Michael P. Czech²

¹Department of Medicine and ²Program in Molecular Medicine, University of Massachusetts (UMass) Medical School, Worcester, Massachusetts, USA. ³Department of Surgery, St. Elizabeth's Medical Center, Brighton, Massachusetts, USA.

Epicardial adipose tissue (EAT) is the visceral fat depot of the heart. Inflammation of EAT is thought to contribute to coronary artery disease (CAD). Therefore, we hypothesized that the EAT of patients with CAD would have increased inflammatory gene expression compared with controls without CAD. Cardiac surgery patients with ($n = 13$) or without CAD ($n = 13$) were consented, and samples of EAT and subcutaneous adipose tissue (SAT) were obtained. Transcriptomic analysis was performed using Affymetrix Human Gene 1.0 ST arrays. Differential expression was defined as a 1.5-fold change (ANOVA $P < 0.05$). Six hundred ninety-three genes were differentially expressed between SAT and EAT in controls and 805 in cases. Expression of 326 genes was different between EAT of cases and controls; expression of 14 genes was increased in cases, while 312 were increased in controls. Quantitative reverse transcription PCR confirmed that there was no difference in expression of CCL2, CCR2, TNF- α , IL-6, IL-8, and PAI1 between groups. Immunohistochemistry showed more macrophages in EAT than SAT, but there was no difference in their number or activation state between groups. In contrast to prior studies, we did not find increased inflammatory gene expression in the EAT of patients with CAD. We conclude that the specific adipose tissue depot, rather than CAD status, is responsible for the majority of differential gene expression.

Introduction

Obesity is a known risk factor for type 2 diabetes mellitus (T2DM). T2DM conveys increased risk for the development of cardiovascular disease (CVD). In fact, diabetes mellitus is considered a “risk equivalent” of established CVD itself (1). Obese people with visceral, rather than subcutaneous, adiposity are at greater risk for the development of T2DM and incident CVD. In the setting of chronic caloric excess, an inflammatory response is initiated in visceral adipose tissue (VAT) (2). The stimulus for this inflammatory response remains unknown. VAT inflammation results in adipocyte dysfunction, including failure to store free fatty acids as triglyceride and increased lipolysis. Excess free fatty acids are released into the circulation and deposited in ectopic tissues, such as the liver, skeletal muscle, heart, and pancreas. Ectopic lipid storage results in insulin resistance in target organs (2, 3). This paradigm has dominated our understanding of T2DM since the 1990s (4, 5). It follows that antiinflammatory therapies would be beneficial in the treatment of T2DM and the prevention of CVD, yet the success of antiinflammatory therapies in the treatment of cardiometabolic disorders has been limited (6).

The ability of VAT to stimulate this cycle of inflammation and insulin resistance is underscored by the syndrome of “normal-weight” obesity: patients with normal BMIs but increased waist circumference and disproportionately increased VAT (7). Despite having a normal BMI these patients are prone to insulin resistance and T2DM because of excess VAT. These observations have led to interest in the direct adverse effects of VAT on neighboring organs. For example, epicardial adipose tissue (EAT) is the visceral fat depot of the heart (8). Modest amounts of EAT are present in normal-weight humans; in overweight humans the amount of EAT increases proportionately with obesity and VAT (9). EAT is contained within the visceral pericardium and supports the epicardial coronary arteries and great cardiac veins (8). Early studies by Mazurek et al. demonstrated that EAT surrounding atherosclerotic coronary arteries had increased expres-

Conflict of interest: The authors have declared that no conflict of interest exists.

Copyright: © 2019, Fitzgibbons et al. This is an open access article published under the terms of the Creative Commons Attribution 4.0 International License.

Submitted: September 11, 2018

Accepted: September 5, 2019

Published: October 17, 2019.

Reference information: *JCI Insight*. 2019;4(20):e124859.
<https://doi.org/10.1172/jci.insight.124859>.

sion of inflammatory genes and dense inflammatory cell infiltrates compared with subcutaneous adipose tissue (SAT) (10). This observation suggested that inflammation of EAT may contribute to or exacerbate atherosclerosis in the underlying coronary artery. Many other groups have replicated these results, finding increased inflammatory gene expression in the EAT of patients with coronary artery disease (CAD) (11–14). However, there are some limitations to these prior studies. First, control patients without CAD were not routinely included. This is important because inflammation in VAT is typically greater than SAT even in normal conditions (15). Second, it is impossible to discern the temporal relationship between the development of CAD and inflammation in adjacent EAT. Therefore, to address some of these limitations, we chose to directly compare gene expression in the EAT of patients with and without CAD.

We hypothesized that inflammatory gene expression would be greater in the EAT of patients with CAD. Contrary to our hypothesis, we found a greater number of genes differentially expressed in the EAT of patients *without* CAD. In particular, we found increased expression of all 3 members of the NR4A subfamily of orphan nuclear hormone receptors (*NR4A1*, *NR4A2*, *NR4A3*) in the EAT of those without CAD. Members of this subfamily have been found to suppress inflammatory gene expression (16, 17). For example, whole-body and macrophage-specific deletion of *Nr4a1* in mice results in a worsening of atherosclerosis (17, 18). Therefore, we conclude that the development of CAD may be associated with *decreased antiinflammatory* gene expression in EAT. Promotion of antiinflammatory effects via pharmacological activation of the orphan nuclear hormone receptors may be advantageous in the treatment of CAD and other cardiometabolic disorders and will be the focus of future studies.

Results

Clinical characteristics. The clinical characteristics of subjects are shown in Table 1. There was no difference in age, gender, BMI, comorbid conditions, or pertinent medication use. The mean age of controls was 67.1 ± 9.9 years and cases 65.3 ± 13.0 years ($P = 0.70$). There was a trend toward more female patients in the control group (46% vs. 23% for cases, $P = 0.41$). The mean Gensini score was 0.7 ± 1.3 in controls and 53.7 ± 27.2 in cases ($P < 0.001$). Therefore, with the exception of the presence of CAD, our study groups were well matched.

EAT contains smaller adipocytes and is more vascularized. We first compared the histological characteristics of SAT and EAT. Both SAT and EAT contained unilocular white adipocytes (Figure 1); no brown adipocytes were visualized. Control SAT adipocytes were significantly larger than those in EAT ($5213 \pm 1024 \mu\text{m}^2$ vs. $3904 \pm 1241 \mu\text{m}^2$, $P < 0.01$) (Figure 1). This relationship was also seen in cases ($5136 \pm 1058 \mu\text{m}^2$ vs. $3920 \pm 612 \mu\text{m}^2$, $P < 0.01$). There was no difference between cases and controls in depot-specific adipocyte size. We then used an endothelial-specific antibody (von Willebrand factor) to compare the number of blood vessels in SAT and EAT (Figure 1). EAT had a greater number of blood vessels than SAT; this was true for cases (2.2 ± 1.67 vs. 0.66 ± 0.58 per HPF, $P < 0.01$) and controls (2.2 ± 1.29 vs. 0.89 ± 0.72 per HPF, $P < 0.01$). There was no difference between cases and controls in depot-specific blood vessel number.

Microarray analysis demonstrates predominantly depot-specific differences in gene expression. We then compared gene expression in SAT and EAT in control patients. Despite the absence of significant CAD, there were large differences in gene expression between SAT and EAT (Figure 2 and Supplemental Table 1; supplemental material available online with this article; <https://doi.org/10.1172/jci.insight.124859DS1>). In total, 693 genes were differentially expressed ($FC > 1.5$; $P < 0.05$). Expression of 383 genes was increased in EAT and 310 were increased in SAT. We then performed gene set enrichment analysis (GSEA) of differentially expressed genes in both depots. SAT was enriched for expression of genes encoding proteins related to the renin-angiotensin system, neuroactive receptor-ligand interactions, and many biochemical pathways (insulin signaling, starch, sucrose, and butanoate metabolism) (Figure 2C). In contrast, EAT was enriched for expression of genes encoding inflammatory pathways, such as complement and coagulation cascades, focal adhesion, and cytokine-receptor interaction (Figure 2C).

In patients with CAD 805 genes were differentially expressed between SAT and EAT (Figure 3 and Supplemental Table 1). Expression of 427 was increased in EAT and 328 in SAT. GSEA demonstrated that SAT was enriched for expression of genes encoding proteins implicated in the renin-angiotensin system, nicotinate and nicotinamide metabolism, and TGF- β signaling pathways (Figure 3C). Similar to control patients, EAT was enriched for expression of genes encoding proteins belonging to complement and coagulation cascades, cell adhesion molecules, focal adhesion and calcium signaling pathways (Figure 3C).

We then directly compared the gene expression profile of EAT in cases and controls (Figure 4). Three hundred twenty-six genes were differentially regulated (1.5-fold change, $P < 0.01$). Expression of 312 genes

Table 1. Clinical characteristics of study participants

	Controls (n = 13)	Cases (n = 13)	P value
Age	67.1 ± 9.9	65.3 ± 13.0	0.70
Female	6 (46%)	3(23%)	0.41
BMI (kg/m ²)	31.75 ± 5.7	29.5 ± 6.3	0.37
Hypertension	9 (69.2%)	9 (69.2%)	0.99
CHF	6 (46.1%)	4 (30.7%)	0.68
Diabetes mellitus	3 (23.0%)	4 (30.7%)	0.99
COPD	0 (0%)	2 (15.4%)	0.48
Chronic kidney disease	1 (7.7%)	2 (15.4%)	0.99
Hyperlipidemia	9 (69.2%)	10 (76.9%)	0.99
Obese	7 (53.8%)	4 (30.8%)	0.41
Gensini score	0.7 ± 1.3	53.7 ± 27.2	<0.001
Statins	6 (46%)	7 (53%)	0.99
Ejection fraction (%)	54.8 ± 18.1	53.22 ± 16.3	0.82
HbA1c%	6.0 ± 0.8	6.3 ± 0.9	0.48
TC (mg/dL)	179.3 ± 54.6	153.4 ± 47.6	0.31
LDL (mg/dL)	108.0 ± 41.9	88.8 ± 33.3	0.28
HDL (mg/dL)	45.7 ± 15.0	41.6 ± 13.5	0.54
TG (mg/dL)	119.6 ± 42.3	115.1 ± 6.0	0.86

CHF, congestive heart failure; COPD, chronic obstructive pulmonary disease; HbA1c%, hemoglobin A1c; TC, total cholesterol; LDL, low-density lipoprotein-cholesterol; HDL, high-density lipoprotein-cholesterol; TG, triglycerides.

was increased in controls and 14 in cases (Figure 4A, Table 1, and Supplemental Table 1). Because of the small number of genes differentially regulated in the EAT of cases, no Kyoto Encyclopedia of Genes and Genomes (KEGG) pathway was significantly enriched in this depot (Figure 4C). However, several pathways were increased in the EAT of controls, including olfactory transduction, pentose and glucuronate interconversion, and Toll-like receptor transduction (Figure 4C).

We then compared gene expression in SAT between cases and controls (Figure 5). Expression of 218 genes was significantly different; expression of 82 was increased in the SAT of controls and 136 in the SAT of cases (Figure 5A). No pathways were significantly enriched in the SAT of controls; several pathways were increased in the SAT of cases, including those encoding proteins implicated in circadian rhythms, chemokine signaling, and NOD receptor signaling (Figure 5C).

Finally, an advantage of the Human Gene 1.0 array is that it contains probes for MIRs. Therefore, we used this feature to compare MIR expression in SAT and EAT in cases and controls (Table 2 and Table 3). Expression of MIRs 126 and 1247 was significantly upregulated in the EAT of controls and cases compared with respective SAT. MIR24-2 expression was increased in the SAT of cases and controls in comparison with EAT.

Therefore, contrary to our expectations, microarray analysis did not demonstrate greater inflammatory gene expression in the EAT of cases in comparison to controls. Rather, depot-specific differences predominated, with SAT of both cases and controls enriched in certain pathways (renin-angiotensin system, focal adhesion) and EAT of both cases and controls enriched in others (complement and coagulation, calcium signaling) (Figure 2 and Figure 3).

Quantitative reverse transcription PCR and immunohistochemistry show that there is no difference in inflammation between EAT of cases and controls. We performed quantitative reverse transcription (qRT-PCR) to verify the expression patterns that we observed in the microarray experiments. First, we showed that our samples displayed a depot-specific identity. EAT of both cases and controls had a higher expression of the visceral fat marker omentin-1 (*INTLN1*) (Figure 6A). In contrast, the SAT of cases and controls expressed higher levels of the subcutaneous fat marker neuronatin (*NNAT*) (Figure 6B). Expression of common inflammatory genes (*CCR2*, *CCL2*, *IL8*, *IL6*, *PAI1*, and *TNFA*) was not significantly different between groups (Figure 6). Interestingly, expression of 3 members of the orphan nuclear hormone receptor family was increased in the EAT of control patients in comparison with cases (Figure 6, C–E).

We then performed immunohistochemistry for markers of classical (M1) and alternative (M2) macrophage activation. In both cases and controls, EAT had a significantly greater number of classical (CD11c⁺) and alterna-

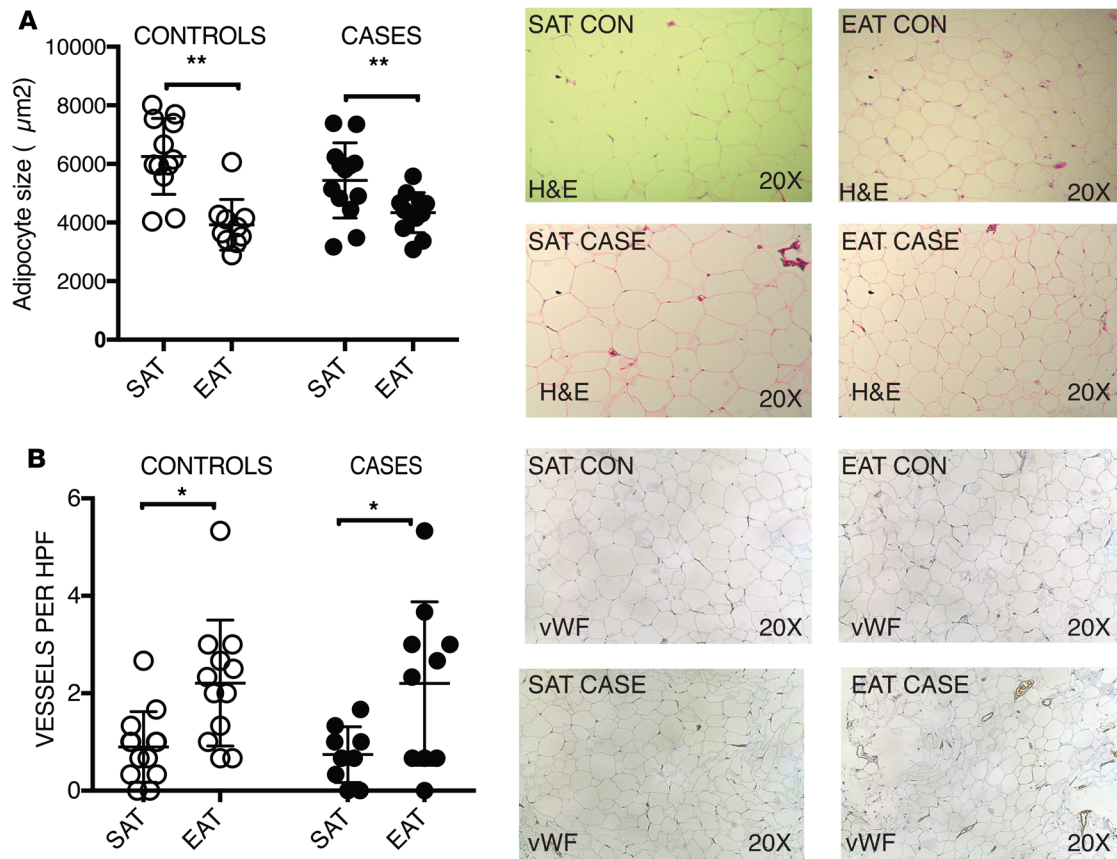


Figure 1. EAT contains smaller adipocytes and greater number of blood vessels. (A) Adipocyte size was determined using Adiposoft software on H&E-stained sections of SAT and EAT in both cases and controls (top right). The mean adipocyte size in SAT was larger than those in EAT (top left). This was true for both cases and controls. (** $P < 0.01$ SAT vs. EAT, 2-tailed Student's t test; $n = 13$ per group. In each column, individual subjects are plotted, and error bars show the mean and standard deviation per group). **(B)** Sections of SAT and EAT were stained with vWF, and the number of blood vessels per high-power field (HPF) was quantified (bottom right). EAT had more blood vessels per field than SAT. (* $P < 0.05$ EAT vs. SAT, 2-tailed Student's t test; $n = 13$ per group. In each column, individual subjects are plotted, and error bars show the mean and standard deviation per group).

tive (mannose receptor C-type 1–positive [MRC1⁺]) macrophages than SAT (Figure 7). There was no difference in the number of positive-stained cells between the EAT of cases and controls (Figure 7). Furthermore, we did not observe a difference in the ratio of M1/M2 cells per depot or on a disease-specific basis (Figure 7E).

Discussion

There has been much recent interest in the potential role of EAT as a direct link between obesity and CAD (19, 20). Initial studies showed that EAT had greater mRNA and protein expression of inflammatory genes and clusters of inflammatory cells (10, 21). Subsequent analyses have demonstrated that EAT tends to have a more inflammatory gene expression profile than SAT, and this is true even in the absence of CAD (12–14). The majority of the data suggest that EAT is very similar to abdominal VAT in that it tends to be more immunologically active than SAT even in normal conditions. There may be an additional increase in inflammation in the setting of atherosclerosis, but it is the adipose organ itself, not the disease state, that dictates the majority of differences in gene expression (13, 14). This concept was originally proposed by Chatterjee et al. in 2009 (22).

Our study confirms many of these findings and makes several potentially novel observations. First, we confirmed that type of adipose tissue, rather than the disease condition, is responsible for most of the differences in gene expression. Six hundred ninety-three genes were differentially expressed between SAT and EAT in controls and 805 in cases. In particular, there is a hallmark panel of genes whose expression is consistently increased in EAT (*INTLN1*, *SYT4*, *CFB*, *ESR*, *INMT*, *PRG4*, and *ALOX15*) compared with SAT irrespective of the presence or absence of CAD (13). In contrast, when directly comparing the EAT of cases and controls, there are fewer differences in gene expression (326 probes different). However, among

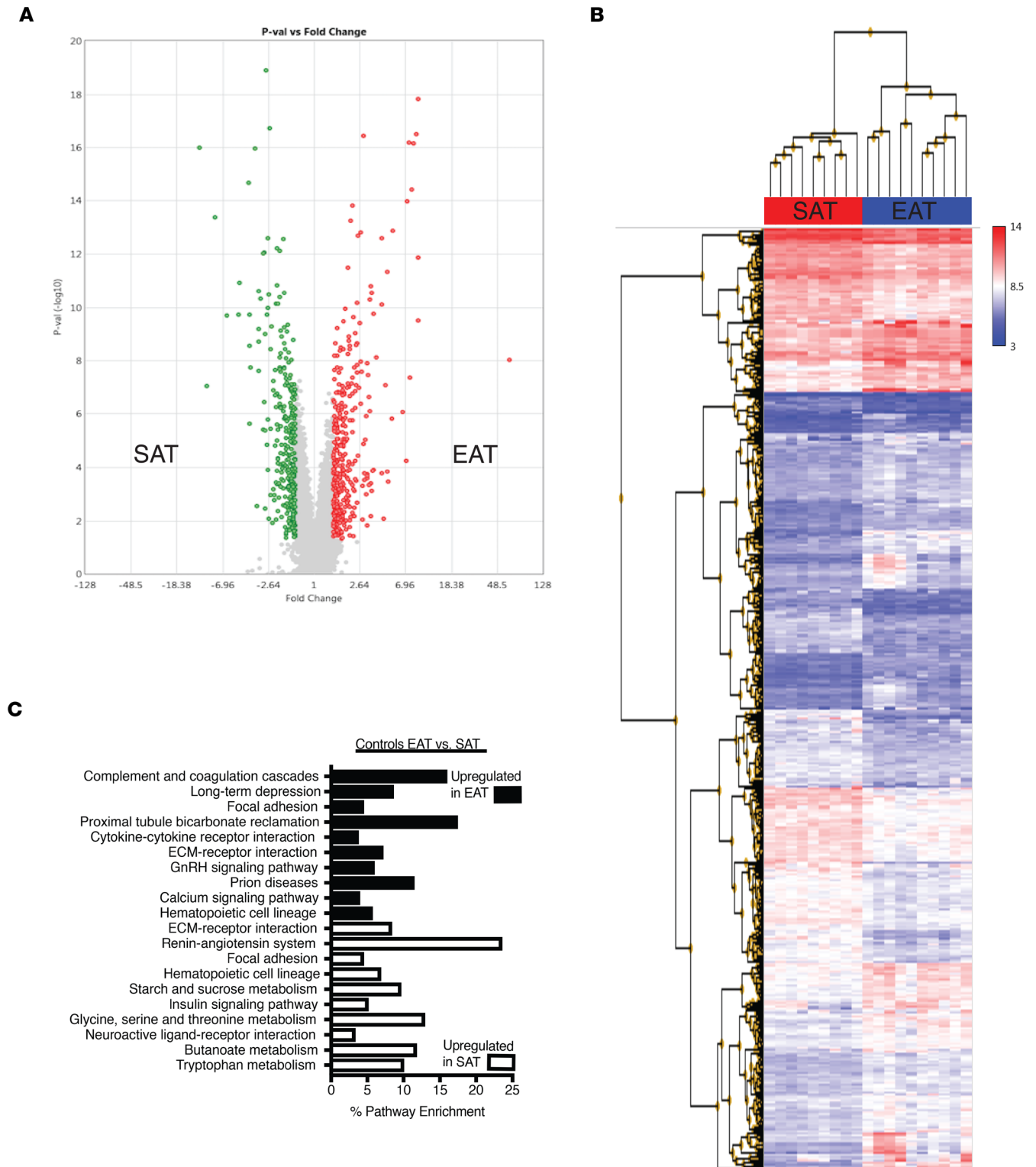


Figure 2. Comparison of gene expression between SAT and EAT in controls. (A) Volcano plot of 693 probes that were differentially expressed at a level of 1.5-fold change (FC) (ANOVA $P < 0.05$). In EAT (shown in red), 383 were upregulated, and 310 were upregulated in SAT (shown in green). (B) Hierarchical clustering of differentially expressed genes in control SAT and EAT. (C) KEGG pathway analysis of differentially expressed genes in SAT and EAT.

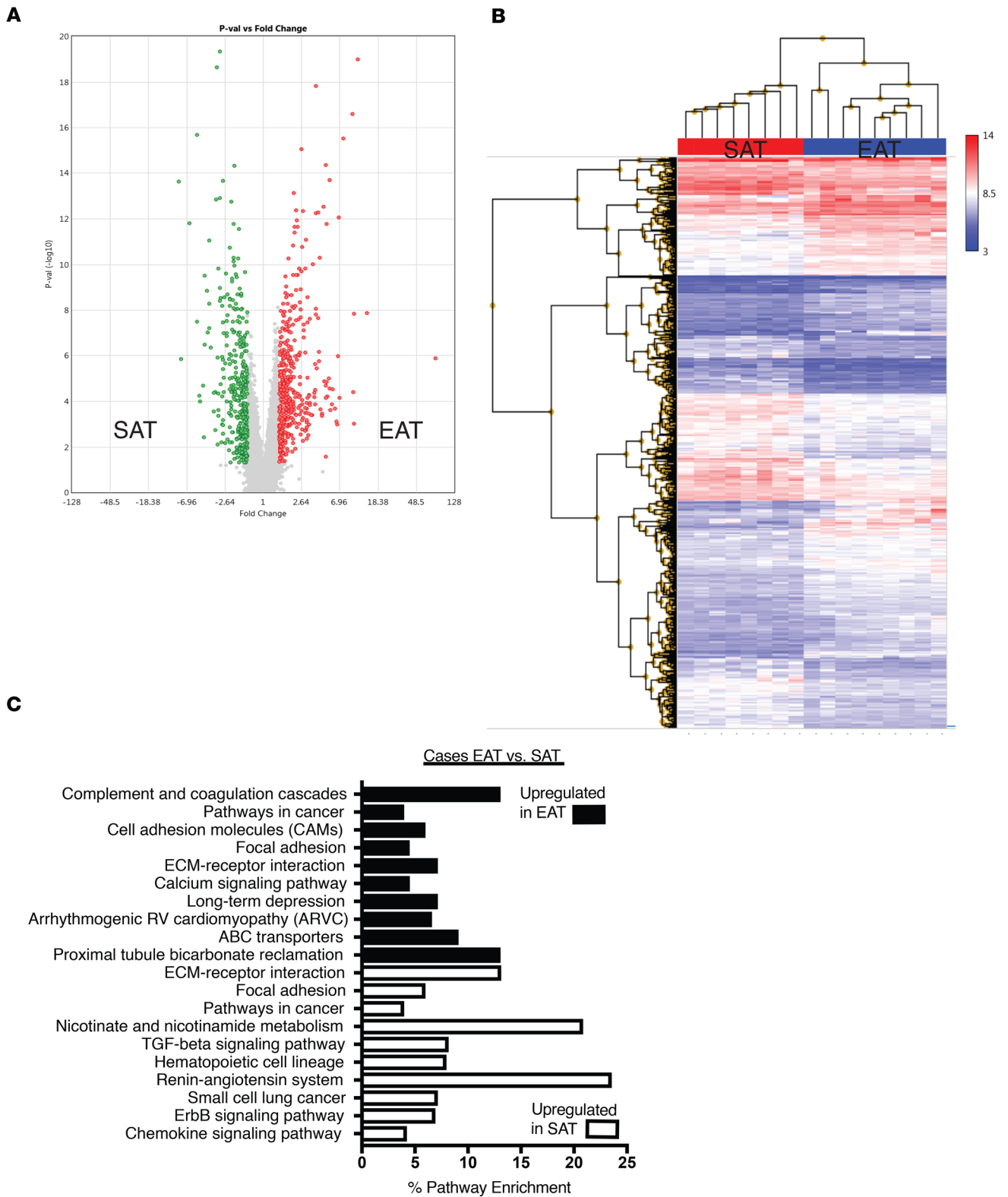


Figure 3. Comparison of gene expression between SAT and EAT in cases. (A) Volcano plot of 805 genes that were differentially expressed at a level of 1.5-fold change (ANOVA $P < 0.05$). In EAT (red) 427 were upregulated, and 378 were upregulated in SAT (green). **(B)** Hierarchical clustering of differentially expressed genes in SAT and EAT of cases. **(C)** KEGG pathway analysis of differentially expressed genes in SAT and EAT of cases.

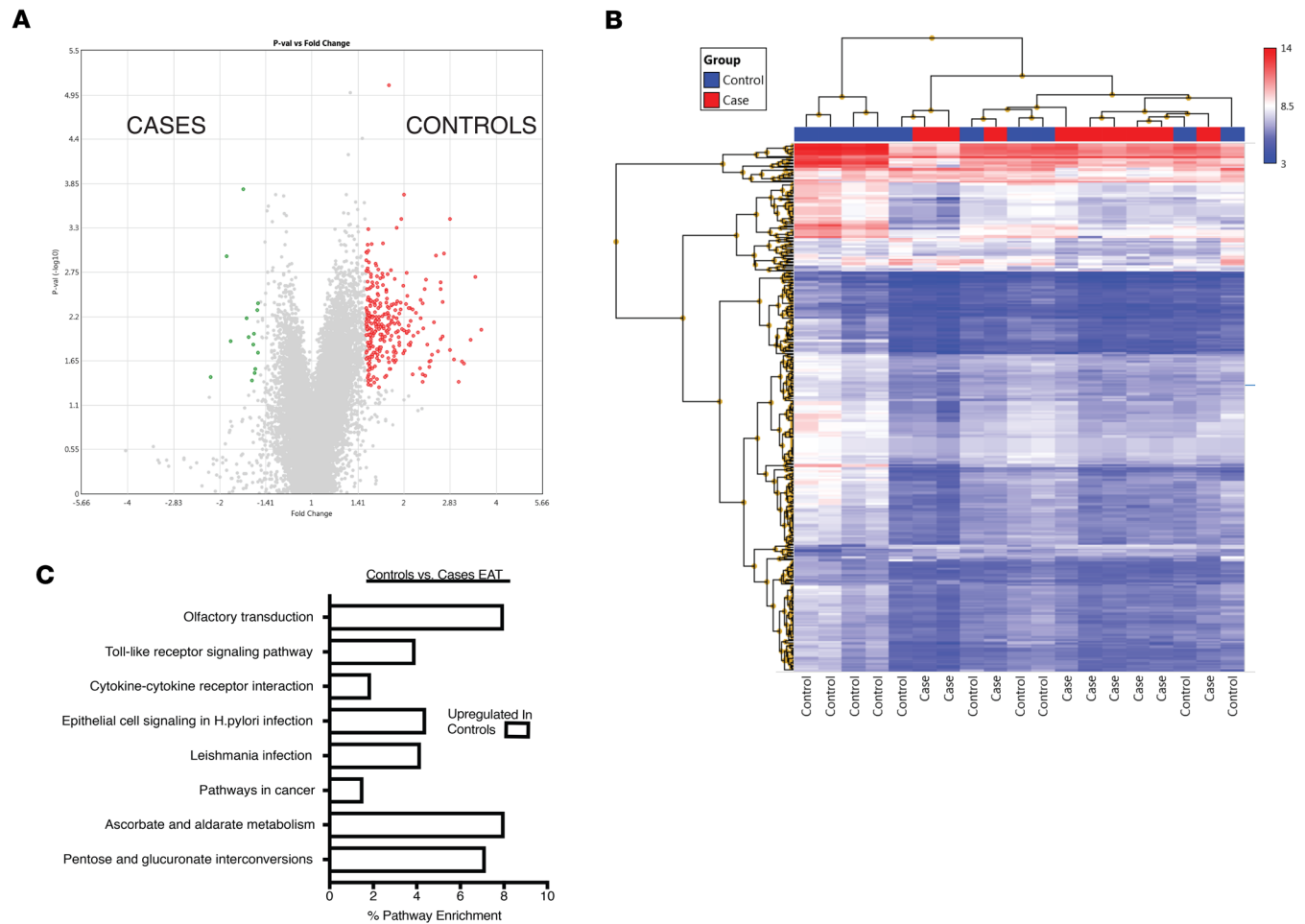


Figure 4. Comparison of gene expression in EAT between cases and controls. (A) Volcano plot of 326 genes that were differentially expressed at a level of 1.5-fold change (ANOVA $P < 0.05$). Three hundred twelve were upregulated in the EAT of control patients (red) and 14 in the EAT of cases (green). **(B)** Hierarchical clustering of differentially expressed genes in EAT of cases and controls. **(C)** KEGG pathway analysis of differentially expressed genes in EAT of controls. No pathways were significantly enriched in the EAT of cases.

these differences, we found that expression of 3 members of the NR4A subfamily of orphan nuclear hormone receptors was increased in the EAT of patients *without* CAD. This has not been previously reported to our knowledge and is very interesting considering that members of this family have been shown to be protective in mouse models of atherosclerosis (17, 18).

The NR4A subfamily of orphan nuclear hormone receptors belong to the same class of transcription factors as peroxisome proliferator-activated receptor γ . Their protein structure is similar to other members in this class, having separate DNA- and ligand-binding domains. They are called “orphan” receptors because their endogenous ligands have yet to be discovered. NR4A family members are expressed in a broad array of tissues and have been shown to protect against the initiation and progression of atherosclerosis (23, 24). Recent studies have highlighted *NR4A1* as a key transcriptional regulator of lipid homeostasis, vascular remodeling, and inflammation (25). *NR4A1* has at least 3 important antiinflammatory effects relevant to CAD. First, NR4A1 activity is required for the differentiation of Ly6c⁻ monocytes that patrol the endothelium and maintain blood vessel integrity. Nr4a1-null mice lack this antiinflammatory monocyte population and display an exaggerated inflammatory response (16, 17). Second, within Ly6c⁺ monocytes, Nr4a1 feeds back to inhibit inflammasome activity and transactivation of NF- κ B by IL-2. Third, Nr4a1 suppresses induction of macrophage chemotactic protein-1 expression in response to lipopolysaccharide (22). Although we do not know the specific cell type responsible for NR4A1 expression in EAT, we hypothesize that it is macrophages. Hirata et al. reported that the ratio of M2 (alternatively activated) to M1 (classically activated) macrophages is greater in the EAT of patients without CAD (21). The inflammatory

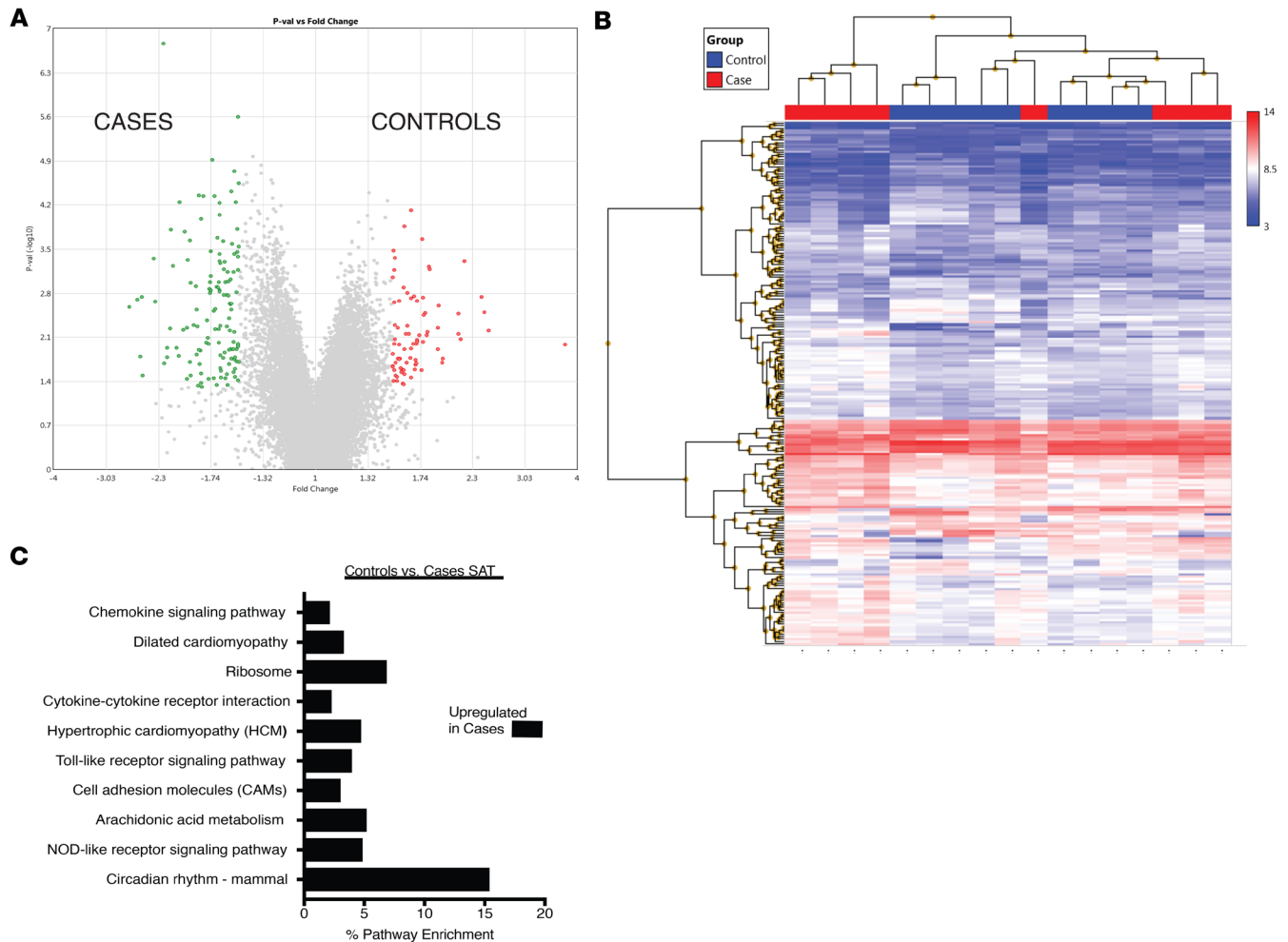


Figure 5. Comparison of gene expression in SAT between cases and controls. (A) Volcano plot of 218 genes that were differentially expressed at a level of 1.5-fold change (ANOVA $P < 0.05$). Eighty-two were upregulated in the SAT of control patients (red) and 136 in the SAT of cases (green). **(B)** Hierarchical clustering of differentially expressed genes in SAT of cases and controls. **(C)** KEGG pathway analysis of differentially expressed genes in SAT of cases. No pathways were significantly enriched in the SAT of controls.

phase of myocardial infarction (MI) is characterized by influx of Ly6c^{hi}CCR2^{hi} monocytes (27). The transition to the reparative phase of MI is dependent upon NR4A1 downregulation of inflammatory cytokine production and transition to Ly6c^{lo}CCR2^{lo} macrophages. Deletion of NR4A in this context leads to excessive inflammation and maladaptive post-MI remodeling (27). Therefore, we hypothesize that within the EAT of patients without CAD, there exists a greater population of antiinflammatory macrophages. Determining whether this is true will require further research.

We showed that epicardial adipocytes are smaller than subcutaneous adipocytes, which is consistent with their visceral lineage. This confirms work by prior authors (28). We did not, however, see a difference in the size of epicardial adipocytes between cases and controls; this is in contrast to the work of Vianello et al., who demonstrated that epicardial adipocyte size was greater in patients with CAD than in those without (29). We hypothesize that this could be due to differences in the patient population. Vianello et al. included only male patients in their study, and the average BMI of patients in their study was lower (29).

A potentially novel finding in our study is that EAT appears to have a greater number of blood vessels than SAT. This has not been previously shown. This was unexpected because visceral adipose depots have previously been demonstrated to have a lower blood vessel density than SAT (30). However, it may be that EAT is different from abdominal VAT in this regard. Furthermore, EAT is known to have a blood supply from the underlying coronary arteries; therefore it follows that there may be a higher vascularity in this adipose depot, which is in close proximity to the heart (8).

Table 2. Differential microRNA expression in SAT and EAT of controls

ID	Control EAT avg (log ₂)	Control SAT avg (log ₂)	FC	ANOVA P value	Gene Symbol	Description
8159371	5.19	4.41	1.72	0.0005	MIR126	microRNA 126
7981326	8.07	7.38	1.61	5.81E-10	MIR1247	microRNA 1247
8034694	6.07	6.68	-1.53	0.0239	MIR24-2	microRNA 24-2

MIR, microRNA.

Interestingly, we found that the expression level of MIR126 was higher in the EAT of both cases and controls compared with SAT. MIR126 is one of the most abundant MIRs in endothelial cells (31). MIR126 promotes regeneration of endothelial cells and regulates endothelial cell turnover (32). The increased expression of this MIR in EAT is consistent with the increased number of endothelial cells in this depot.

Our study has several limitations. First, we have a modest number of patients. Second, we could not obtain samples of visceral fat to compare the 3 depots. Third, samples of EAT were obtained proximal to the right coronary artery only, because this is the easiest area for the surgeon to take the biopsy from. These limitations aside, we feel that we have made some potentially novel observations regarding the characteristics of EAT that add to the present literature.

Conclusions. We conclude that the adipose depot, rather than disease status, is the predominant determinant of gene expression in EAT. EAT has greater inflammatory gene expression than SAT even in the absence of coronary disease; this is consistent with its visceral origin. Regarding disease-specific gene expression, patients without coronary disease had higher expression of all 3 members of the orphan nuclear hormone receptor family in EAT. This is consistent with mouse studies demonstrating a protective and antiinflammatory effect of these nuclear receptors in atherosclerosis. We hypothesize that these receptors may play an important role in limiting adipose tissue inflammation in cardiometabolic disorders.

Methods

Subject recruitment. Adult patients referred for elective cardiac surgery were screened for enrollment and informed consent was provided. This study was approved by the UMass IRB (docket H-14436). Patients with active infection or cancer were excluded. All patients had preoperative coronary angiography. Control patients were referred for elective valve surgery and had no significant CAD (any single lesion >50%) on preoperative coronary angiograms. Only 3 controls had single lesions of 30%; otherwise, all had normal coronary arteries or minor luminal irregularities. Cases were patients referred for coronary artery bypass surgery because of significant CAD. The severity of CAD was determined by single-blinded review of coronary angiograms and calculation of the Gensini score as previously described (33). The Gensini score is a continuous variable that increases with the severity of coronary atherosclerosis (e.g., a score of 0 = none, and 100 = severe).

Table 3. Differential microRNA expression in SAT and EAT of cases

ID	Control EAT avg (log ₂)	Control SAT avg (log ₂)	FC	ANOVA P value	Gene Symbol	Description
7981326	8.08	7.26	1.76	1.78E-09	MIR1247	microRNA 1247
8159371	5.28	4.67	1.52	0.0072	MIR126	microRNA 126
8067944	6.27	5.67	1.52	0.0011	MIRLET7C	microRNA let-7c
8011193	8.44	9.02	-1.5	9.73E-08	MIR22	microRNA 22
8034698	7.48	8.18	-1.62	0.0012	MIR23A	microRNA 23a
8054611	8.43	9.17	-1.68	5.05E-06	MIR4435	microRNA 4435
8172266	6.2	7.17	-1.96	1.15E-05	MIR221	microRNA 221
8008885	7.65	9.29	-3.12	4.47E-05	MIR21	microRNA 21
8034694	5.27	7.57	-4.94	9.98E-05	MIR24-2	microRNA 24-2

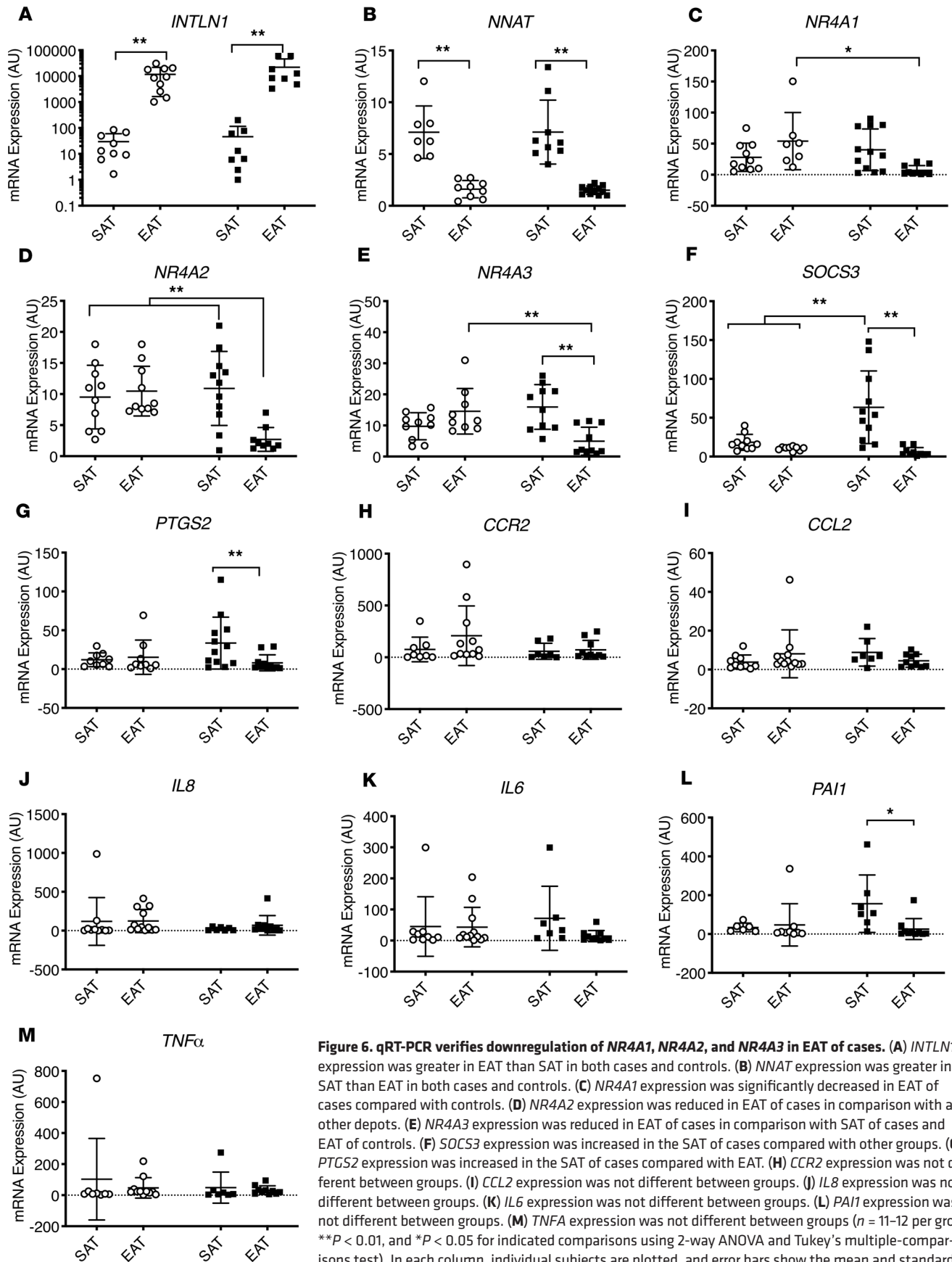


Figure 6. qRT-PCR verifies downregulation of NR4A1, NR4A2, and NR4A3 in EAT of cases. (A) *INTLN1* expression was greater in EAT than SAT in both cases and controls. (B) *NNAT* expression was greater in SAT than EAT in both cases and controls. (C) *NR4A1* expression was significantly decreased in EAT of cases compared with controls. (D) *NR4A2* expression was reduced in EAT of cases in comparison with all other depots. (E) *NR4A3* expression was reduced in EAT of cases in comparison with SAT of cases and EAT of controls. (F) *SOCS3* expression was increased in the SAT of cases compared with other groups. (G) *PTGS2* expression was increased in the SAT of cases compared with EAT. (H) *CCR2* expression was not different between groups. (I) *CCL2* expression was not different between groups. (J) *IL8* expression was not different between groups. (K) *IL6* expression was not different between groups. (L) *PAI1* expression was significantly higher in SAT of cases compared with EAT (*). (M) *TNFA* expression was not different between groups ($n = 11-12$ per group; $**P < 0.01$, and $*P < 0.05$ for indicated comparisons using 2-way ANOVA and Tukey's multiple-comparisons test). In each column, individual subjects are plotted, and error bars show the mean and standard deviation per group. White circles represent controls; black squares represent cases.

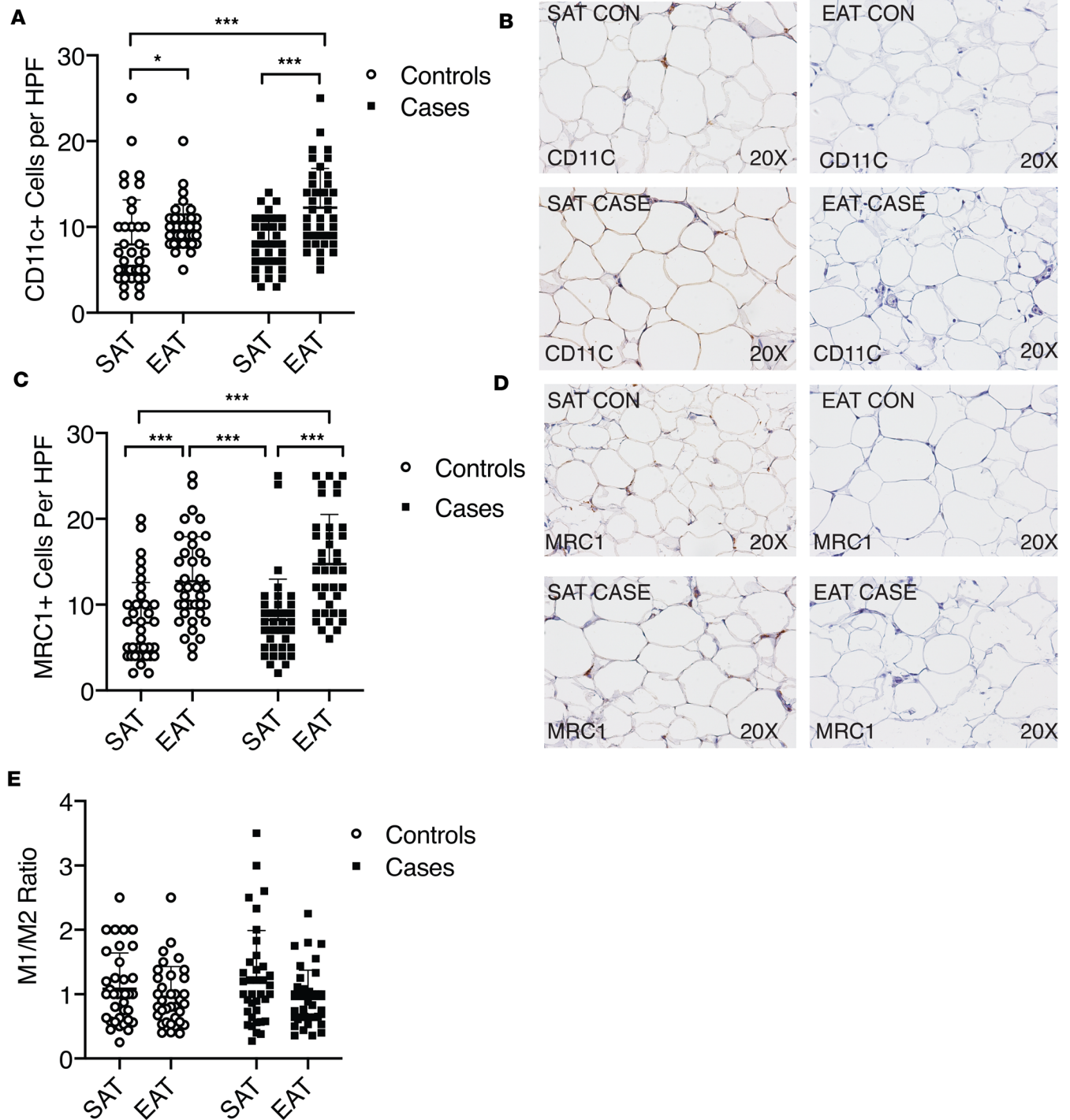


Figure 7. Staining of EAT for classical and alternative macrophage markers shows no difference between cases and controls. (A) Staining of EAT for the classical macrophage marker CD11c showed no difference between cases and controls. EAT of both cases and controls had more CD11c⁺ cells than SAT. * $P < 0.05$; *** $P < 0.001$ vs. EAT for indicated comparisons using Kruskal-Wallis test with Dunn's multiple-comparisons test. In each column, individual subjects are plotted, and error bars show the mean and standard deviation per group. (B) Representative CD11c staining in cases and controls. (C) Staining of EAT for the alternative macrophage marker MRC1 showed no difference between cases and controls. EAT of both cases and controls had a greater number of MRC1⁺ cells than SAT. *** $P < 0.001$ vs. EAT for indicated comparisons using Kruskal-Wallis test with Dunn's multiple-comparisons test. In each column, individual subjects are plotted, and error bars show the mean and standard deviation per group. (D) Representative MRC1 staining in cases and controls. (E) The average values of CD11c and MRC1⁺ cells per subject and tissue were divided to create a ratio. There was no difference in the ratio per tissue or group using Kruskal-Wallis test.

Sample collection and preparation. During surgery a sample of EAT (0.5 g) adjacent to the right coronary artery was obtained, a section was taken and stored in 10% formalin, and the remainder was immediately snap-frozen in liquid nitrogen (-80°C). Next, a sample of SAT (0.5 mg) from thoracic subcutaneous fat was obtained, a section was taken and stored in 10% formalin, and the remainder was immediately snap-frozen in liquid nitrogen (-80°C).

Microarray analysis. RNA was prepared from aliquots of frozen fat samples using the QIAGEN mini lipid RNA extraction kit. RNA quality was analyzed on an Agilent Bioanalyzer. Samples with an RNA integrity number below 7.5 were excluded. Samples that passed quality control analysis were sent to the UMass Genomics Core for cRNA preparation and hybridization to Affymetrix Human Gene 1.0 Arrays. Expression analysis was performed using Affymetrix Transcriptome Analysis Software. The raw data were deposited into the National Center for Biotechnology Information's Gene Expression Omnibus database with accession number GSE120774 (<http://www.ncbi.nlm.nih.gov/geo>).

qRT-PCR. qRT-PCR was performed using a cDNA synthesis kit, SYBR Green Master Mix, and a CFX 96 thermocycler (all from Bio-Rad) as previously described (34). Primer sequences were obtained from PrimerBank (<http://pga.mgh.harvard.edu/primerbank>) and were as follows: *CCR2* forward CCA-CATCTCGTTCTCGGTTTATC, *CCR2* reverse CAGGGAGCACCGTAATCATAATC, *CCL2* forward CAGCCAGATGCAATCAATGCC, *CCL2* reverse TGGAAATCCTGAACCCACTTCT, *GAPDH* forward GGAGCGAGATCCCTCCAAAAT, *GAPDH* reverse GGCTGTTGTCATACTTCTCATGG, *IL8* forward TTTTGCCAAGGAGTGCTAAAGA, *IL8* reverse AACCTCTGCACCCAGTTTTTC, *IL6* forward ACTCACCTCTTCAAGCAATG, *IL6* reverse CCATCTTTGGAAGGTTTCAGGTTG, *ITLN1* forward ACGTGCCCAATAAGTCCCC, *ITLN1* reverse CCGTTGTCAGTCCAACACTTTC, *NNAT* forward ACTGGGTAGGATTCGCTTTTTCG, *NNAT* reverse ACACCTCACTTCTCGCAATGG, *NR4A1* forward ATGCCCTGTATCCAAGCCC, *NR4A1* reverse GTGTAGCCGTCCATGAAGGT, *NR4A2* forward GTTCAGGCGCAGTATGGGTC, *NR4A2* reverse CTCCCGAAGAGTGGTAAGTGT, *NR4A3* forward TGCGTCCAAGCCCAATATAGC, *NR4A3* reverse GGTGTATTCCGAGCTGTATGTCT, *PAI1* forward ACCGCAACGTGGTTTTTCTCA, *PAI1* reverse TTGAATCCCATAGCTGCTTGAAT, *PTGS2* forward CTGGCGCTCAGCCATACAG, *PTGS2* reverse CGCACTTATACTGGTCAAATCCC, *SOCS3* forward CCTGCGCTCAAGACCTT, *SOCS3* reverse GTCAGTGCCTCCAGTAGAA, *TNFA* forward CCTCTCTAATCAGCCCTCTG, and *TNFA* reverse GAGGACCTGGGAGTAGATGAG. Expression relative to *GAPDH* was determined using the $\Delta\Delta\text{Ct}$ method of Livak and Schmittgen (35).

Histology and immunohistochemistry. Formalin-fixed sections were embedded in paraffin and sectioned by the UMass Diabetes and Endocrinology Research Center (DERC) Morphology Core. Adipocyte size was determined on H&E-stained sections using the program Adiposoft as previously described (36). To quantify blood vessels, unstained sections were incubated with rabbit anti-human von Willebrand factor (1:300 dilution) (Abcam ab6994) and then a goat antirabbit secondary antibody conjugated to horseradish peroxidase (Pierce 31460). Negative controls using secondary antibody alone were also included. To quantify M1 or M2 macrophages, cryosections were stained with rabbit anti-human CD11c (1:1000 dilution) (abcam ab52632) and rabbit anti-human MRC1 (1:1000 dilution) (abcam ab64693) antibodies and then a goat antirabbit secondary antibody conjugated to horseradish peroxidase. Three representative fields at original magnification $\times 20$ of SAT and EAT of each patient were used to quantify CD11c⁺ and MRC1⁺ cells.

Statistics. Clinical characteristics were compared with the 2-tailed Student's *t* test for continuous variables or the χ^2 test for dichotomous variables. A *P* value less than 0.05 was considered significant. Adipocyte size and endothelial cell numbers were compared with 2-tailed Student's *t* test. For the qRT-PCR experiment, expression values relative to *GAPDH* were compared using 2-way ANOVA and Tukey's multiple-comparisons test. The Affymetrix Transcriptome Analysis Console was used to analyze microarrays using 1-way ANOVA and multiple-comparisons testing.

Study approval. This study was reviewed and approved by the UMass Medical Institutional Review Board (docket H-14436). All studies were conducted according to the principles expressed in the Declaration of Helsinki. Signed informed consent documents were obtained from each participant included in the study.

Author contributions

TPF, SKCT, and MPC conceived and designed the experiments. TPF, NL, KVT, SN, and MK performed the experiments. TPF, NL, KVT, SN, and MK analyzed the data. TPF was responsible for consenting patients, and TPF and SKCT obtained samples. TPF and MPC wrote the paper.

Acknowledgments

This manuscript is dedicated to the memory of John N. Fain. The authors would like to thank the DERC Morphology Core and the UMass Genomics Core for assistance with sample preparation. TPF was supported by American Heart Association grant 12FTF11260010, and MPC was supported by NIH grants DK30898 and DK116056.

Address correspondence to: Timothy P. Fitzgibbons, Division of Cardiovascular Medicine, 55 Lake Avenue North, Worcester, Massachusetts 01655, USA. Phone: 508.856.6573; Email: timothy.fitzgibbons@umassmed.edu.

1. Stone NJ, et al. 2013 ACC/AHA guideline on the treatment of blood cholesterol to reduce atherosclerotic cardiovascular risk in adults: a report of the American College of Cardiology/American Heart Association Task Force on Practice Guidelines. *Circulation*. 2014;129(25 Suppl 2):S1–S45.
2. Guilherme A, Virbasius JV, Puri V, Czech MP. Adipocyte dysfunctions linking obesity to insulin resistance and type 2 diabetes. *Nat Rev Mol Cell Biol*. 2008;9(5):367–377.
3. Czech MP. Insulin action and resistance in obesity and type 2 diabetes. *Nat Med*. 2017;23(7):804–814.
4. Hotamisligil GS, Arner P, Caro JF, Atkinson RL, Spiegelman BM. Increased adipose tissue expression of tumor necrosis factor- α in human obesity and insulin resistance. *J Clin Invest*. 1995;95(5):2409–2415.
5. Weisberg SP, McCann D, Desai M, Rosenbaum M, Leibel RL, Ferrante AW. Obesity is associated with macrophage accumulation in adipose tissue. *J Clin Invest*. 2003;112(12):1796–1808.
6. Pollack RM, Donath MY, LeRoith D, Leibowitz G. Anti-inflammatory agents in the treatment of diabetes and its vascular complications. *Diabetes Care*. 2016;39(Suppl 2):S244–S252.
7. Romero-Corral A, et al. Normal weight obesity: a risk factor for cardiometabolic dysregulation and cardiovascular mortality. *Eur Heart J*. 2010;31(6):737–746.
8. Sacks HS, Fain JN. Human epicardial adipose tissue: a review. *Am Heart J*. 2007;153(6):907–917.
9. Iacobellis G, et al. Echocardiographic epicardial adipose tissue is related to anthropometric and clinical parameters of metabolic syndrome: a new indicator of cardiovascular risk. *J Clin Endocrinol Metab*. 2003;88(11):5163–5168.
10. Mazurek T, et al. Human epicardial adipose tissue is a source of inflammatory mediators. *Circulation*. 2003;108(20):2460–2466.
11. Fain JN, Sacks HS, Bahouth SW, Tichansky DS, Madan AK, Cheema PS. Human epicardial adipokine messenger RNAs: comparisons of their expression in substernal, subcutaneous, and omental fat. *Metab Clin Exp*. 2010;59(9):1379–1386.
12. Guaque-Olarte S, et al. The transcriptome of human epicardial, mediastinal and subcutaneous adipose tissues in men with coronary artery disease. *PLoS One*. 2011;6(5):e19908.
13. Gaborit B, et al. Human epicardial adipose tissue has a specific transcriptomic signature depending on its anatomical peri-atrial, peri-ventricular, or peri-coronary location. *Cardiovasc Res*. 2015;108(1):62–73.
14. Vacca M, et al. Integrative miRNA and whole-genome analyses of epicardial adipose tissue in patients with coronary atherosclerosis. *Cardiovasc Res*. 2016;109(2):228–239.
15. Saddic LA, et al. Joint analysis of left ventricular expression and circulating plasma levels of Omentin after myocardial ischemia. *Cardiovasc Diabetol*. 2017;16(1):87.
16. Hanna RN, et al. The transcription factor NR4A1 (Nur77) controls bone marrow differentiation and the survival of Ly6C-monocytes. *Nat Immunol*. 2011;12(8):778–785.
17. Hanna RN, et al. NR4A1 (Nur77) deletion polarizes macrophages toward an inflammatory phenotype and increases atherosclerosis. *Circ Res*. 2012;110(3):416–427.
18. Hu YW, et al. Nur77 decreases atherosclerosis progression in apoE(-/-) mice fed a high-fat/high-cholesterol diet. *PLoS One*. 2014;9(1):e87313.
19. Brown NK, et al. Perivascular adipose tissue in vascular function and disease: a review of current research and animal models. *Arterioscler Thromb Vasc Biol*. 2014;34(8):1621–1630.
20. Mancio J, Oikonomou EK, Antoniadis C. Perivascular adipose tissue and coronary atherosclerosis. *Heart*. 2018;104(20):1654–1662.
21. Hirata Y, et al. Coronary atherosclerosis is associated with macrophage polarization in epicardial adipose tissue. *J Am Coll Cardiol*. 2011;58(3):248–255.
22. Chatterjee TK, et al. Proinflammatory phenotype of perivascular adipocytes: influence of high-fat feeding. *Circ Res*. 2009;104(4):541–549.
23. Arkenbout EK, et al. Protective function of transcription factor TR3 orphan receptor in atherogenesis: decreased lesion formation in carotid artery ligation model in TR3 transgenic mice. *Circulation*. 2002;106(12):1530–1535.
24. Monajemi H, Arkenbout EK, Pannekoek H. Gene expression in atherogenesis. *Thromb Haemost*. 2001;86(1):404–412.
25. Martínez-González J, Badimon L. The NR4A subfamily of nuclear receptors: new early genes regulated by growth factors in vascular cells. *Cardiovasc Res*. 2005;65(3):609–618.
26. Pols TW, et al. 6-mercaptopurine inhibits atherosclerosis in apolipoprotein e*3-leiden transgenic mice through atheroprotective actions on monocytes and macrophages. *Arterioscler Thromb Vasc Biol*. 2010;30(8):1591–1597.
27. Hilgendorf I, et al. Ly-6Chigh monocytes depend on Nr4a1 to balance both inflammatory and reparative phases in the infarcted myocardium. *Circ Res*. 2014;114(10):1611–1622.
28. Bambace C, et al. Adiponectin gene expression and adipocyte diameter: a comparison between epicardial and subcutaneous adipose tissue in men. *Cardiovasc Pathol*. 2011;20(5):e153–e156.
29. Vianello E, et al. Epicardial adipocyte hypertrophy: Association with M1-polarization and toll-like receptor pathways in coronary artery disease patients. *Nutr Metab Cardiovasc Dis*. 2016;26(3):246–253.

30. Gealekman O, et al. Depot-specific differences and insufficient subcutaneous adipose tissue angiogenesis in human obesity. *Circulation*. 2011;123(2):186–194.
31. Fish JE, et al. miR-126 regulates angiogenic signaling and vascular integrity. *Dev Cell*. 2008;15(2):272–284.
32. Schober A, et al. MicroRNA-126-5p promotes endothelial proliferation and limits atherosclerosis by suppressing Dlk1. *Nat Med*. 2014;20(4):368–376.
33. Gensini GG. A more meaningful scoring system for determining the severity of coronary heart disease. *Am J Cardiol*. 1983;51(3):606.
34. Fitzgibbons TP, Kogan S, Aouadi M, Hendricks GM, Straubhaar J, Czech MP. Similarity of mouse perivascular and brown adipose tissues and their resistance to diet-induced inflammation. *Am J Physiol Heart Circ Physiol*. 2011;301(4):H1425–H1437.
35. Livak KJ, Schmittgen TD. Analysis of relative gene expression data using real-time quantitative PCR and the 2(-Delta Delta C(T)) Method. *Methods*. 2001;25(4):402–408.
36. Galarraga M, et al. Adiposoft: automated software for the analysis of white adipose tissue cellularity in histological sections. *J Lipid Res*. 2012;53(12):2791–2796.